Switchable domains in point contacts based on transition metal tellurides

Yu. G. Naidyuk,[1,*] D. L. Bashlakov,[1] O. E. Kvitnitskaya,[1] B. R. Piening,[2] G. Shipunov,[2] D. V. Efremov,[2,†] S. Aswartham,[2,‡] and B. Büchner[2,3]

[1]*B. Verkin Institute for Low Temperature Physics and Engineering, NAS of Ukraine, 61103 Kharkiv, Ukraine*
[2]*Institute for Solid State Research, IFW Dresden, D-01171 Dresden, Germany*
[3]*Institute of Solid State and Materials Physics, TU Dresden, D-01062 Dresden, Germany*

(Received 22 February 2021; revised 12 July 2021; accepted 29 July 2021; published 16 August 2021)

We report resistive switching in voltage biased point contacts (PCs) based on the van der Waals transition metal tellurides (TMTs) $MeTe_2$ (Me = Mo, W) and $TaMeTe_4$ (Me = Ru, Rh, Ir). The switching occurs between a low resistive "metallic-type" state, which is the ground state, and a high resistive "semiconducting-type" state by applying a certain bias voltage (<1V). The reverse switching takes place by applying voltage of opposite polarity. The origin of the effect can be attributed to the formation of domains with different crystal structure in the PC core due to a strong electric field (>10 kV/cm). The new functionality of the studied TMT materials, which emerges from switchable domains in submicron heterostructures, is very promising, e.g., for nonvolatile resistive random access memory engineering.

DOI: 10.1103/PhysRevMaterials.5.084004

I. INTRODUCTION

Recently, layered van der Waals transition metal chalcogenides (TMCs) have attracted a lot of attention in the scientific community both due to the manifestation of their remarkable electronic properties, which can be modified by element composition, crystal structure, thickness, and electronic density, and for their potential for nanoelectronic and spintronic applications (see [1] and references therein). It was also found that some of them (e.g., $MoTe_2$, WTe_2) are Weyl semimetals possessing massless fermionic excitations and topologically robust electronic surface states [2]. In addition, the layered structure of TMC with a weak van der Waals binding between the layers allows these materials to be exfoliated into monolayers. The latter opens an amazing window to observe new dimensional dependent effects in TMC and allows one to take advantage of this opportunity in future applications [3].

The transition metal telluride (TMT) $MoTe_2$ together with its sister compounds WTe_2 and $TaMeTe_4$ (Me = Ir, Rh, Ru) have recently attracted enormous attention due to their unique physical properties, such as extremely large magnetoresistance [4–6], superconductivity [7–9], higher-order topology [10–12], and the discovery of the polar metallic state [13–17]. It is worth noting that $MoTe_2$ can be grown in two different modifications: as a 2H-phase, which is a semiconductor with a hexagonal crystal structure, and as a T_d and T'-phase, which are semimetals with the crystal structures T_d (at $T < 250$ K) and T' ($T > 250$ K). $TaMeTe_4$ have been realized only in the semimetallic T_d modification so far.

In this study, we have applied the well-established point-contact spectroscopy (PC) technique [18], which allows us to study properties of materials in restricted geometry from submicron to nanometer scale under high current densities and electric fields. A phase transition in the sample may be detected by measuring a nonlinear conductivity of PCs, as was shown, for example, for ferromagnetic metals [19]. Furthermore, the PC technique was recently applied successfully to TMT for investigations of the interface superconductivity and electron-phonon coupling [8,9]. In particular, we found that at the PC the superconducting critical temperature (T_c) in $MoTe_2$ is enhanced by 50 times (up to 5 K) in comparison to the bulk system (0.1 K) [8]. Interestingly, the same strong increase of the superconducting critical temperature in $MoTe_2$ was found in monolayers [20].

In this study, we report our finding of bistable resistive states with reversible switching in current-voltage $I-V$ characteristics of $MoTe_2$ (and related TMT) PCs at biases of several hundreds of millivolts. In contrast to the aforementioned works [13,14], we start with the semimetallic ground state (T_d or T') and transfer the system into a semiconducting-like state. A similar effect has been registered for PCs on related TMTs such as WTe_2 and $Ta_{1.26}Ru_{0.75}Te_4$, $TaRhTe_4$, and $TaIrTe_4$ which were recently synthesized [21]. The observed bipolar resistive switching in devices based on the studied family of TMT compounds, regardless of its inner nature, is of great importance and may be promising to fabricate a new type of resistive random-access memory (RRAM) device as a potential alternative to existing nonvolatile memory devices. Additionally, along with this discovery, understanding the underlying physics of switching processes is of particular interest, while utilizing topological properties and surface states at interfaces in TMTs could pave the way to nanoelectronics with novel functionalities.

II. RESULTS

Figure 1 shows dV/dI and $I-V$ characteristics of "soft" PCs made by adding a small drop of silver paint on the surface

*naidyuk@ilt.kharkov.ua
†d.efremov@ifw-dresden.de
‡s.aswartham@ifw-dresden.de

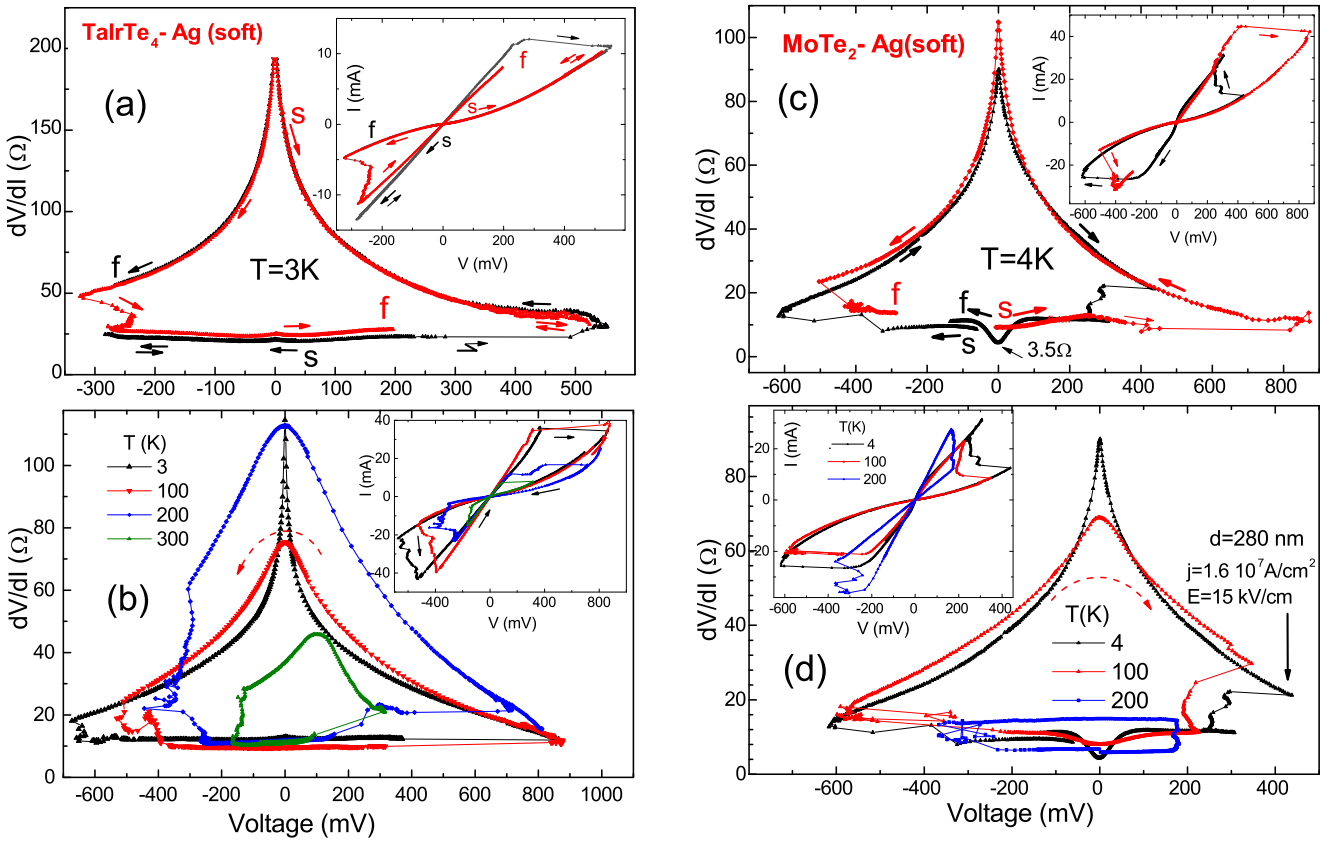

FIG. 1. Differential resistance dV/dI and $I-V$ curve behavior for "soft" contacts based on TMT at different temperatures. (a) dV/dI and $I-V$ curves (inset) of "soft" contacts $TaIrTe_4$-Ag measured at 3 K starting from LRS (black curve) and HRS (red curve). "*s*" marks the starting point of the measurements, and "*f*" is for the finish; arrows show the direction of the current scan. The black curve is measured starting toward negative voltages, forth and back, while transition to HRS occurs only at positive voltages. The red curve is measured starting toward positive voltages, forth and back, while the transition scan to LRS occurs only at negative voltages. (b) dV/dI and $I-V$ curves (inset) of another "soft" contact $TaIrTe_4$-Ag measured at different temperatures. The curves are measured "counterclockwise." (c) dV/dI of two (black and red) "soft" contacts $MoTe_2$-Ag measured starting from LRS. "*s*" marks the starting point of the measurements, and "*f*" is for the finish; arrows show the direction of the current scan. Transition from LRS to HRS (or from HRS to LRS) occurs at opposite polarities for these two contacts. The right inset shows $I-V$ curves corresponding to dV/dI from the main panel. (d) dV/dI and $I-V$ curves (inset) of 3.5 Ω "soft" contact from the panel (c) measured at different temperatures. Note, we usually measured several cycles of the switching loop for each PC, but we do not show extra cycles to make the figures clearer.

of $TaIrTe_4$ and $MoTe_2$ PCs (see Sec. V for more details). A closed loop for dV/dI and a "butterfly" shape for $I-V$ curves are seen by scanning bias voltage from one polarity to the opposite polarity and back. For example, starting from the low resistance state (LRS), switching to the high resistance state (HRS) occurs above +250 mV [Fig. 1(a), black curve], while no switching is observed when scanning the LRS to the opposite negative bias. Starting from the HRS [Fig. 1(a), red curve], where dV/dI demonstrates a sharp zero-bias maximum, the transition to the LRS takes place only at negative polarity, a bit above −300 mV, while at positive polarity no switching to the LRS is observed up to +520 mV.

Figure 1(b) shows dV/dI and $I-V$ characteristics of another "soft" PC based on $TaIrTe_4$ at different temperatures. The switching effect persists up to room temperature, in spite of the fact that the amplitude of the zero bias dV/dI maximum goes down and the switching voltage decreases. Figure 1(c) demonstrates similar dependences for two $MoTe_2$ PCs. Here, the switching from LRS to HRS is at positive polarity for the red curve, as for the PC from Fig. 1(a), while for another PC (black curve) the switching from LRS to HRS (or HRS to LRS) is at negative (positive) polarity. Interestingly, $dI/dV = (dV/dI)^{-1}$ (left inset) displays a clear linear relationship at 4 K.

Figure 1(d) shows the evolution of the dV/dI and $I-V$ (in the inset) characteristics of the latter PC with temperature, where the amplitude of the effect and the switching voltage decreases. The diameter of this PC is estimated as 280 nm using the temperature dependence of the zero bias resistance analogously to the method used in the supplement of Ref. [9]. Using the diameter, we can estimate the strength of the electric field and the current density to be about 15 kV/cm and 1.6×10^7 A/cm^2, respectively, e.g., at the HRS to LRS transition.

Figure 2 shows dV/dI and $I-V$ (in the inset) characteristics of a PC with WTe_2 at room temperature, where the difference in the resistance between LRS and HRS reaches more than two orders of magnitude (see also Fig. S9 in the Supplemental Material [22], where a similar result is shown for the case of $MoTe_2$). There is an instability in the $I-V$ curve at the LRS to HRS transition above 150 mV. The

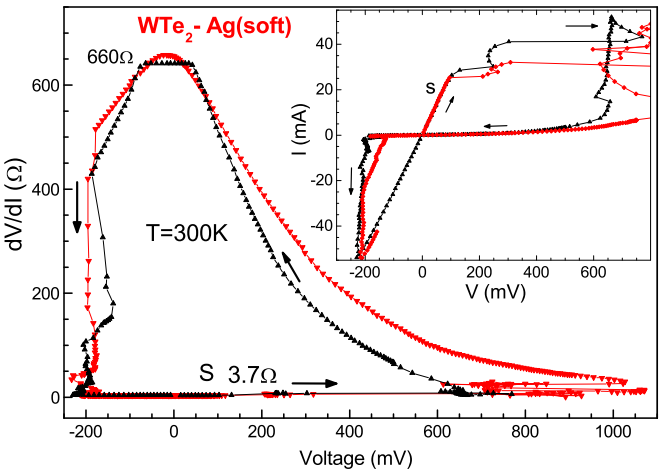

FIG. 2. Differential resistance dV/dI and $I-V$ curve (inset) behavior for "soft" contact based on WTe_2 at room temperature. Two dV/dI of the same "soft" contact WTe_2-Ag measured with a time interval of 12 h at ambient condition. "s" marks the start of measurements, and arrows show the direction of the current scan. Note, the zero bias resistance is changed more than two orders of magnitude. The inset shows the $I-V$ curve corresponding to dV/dI from the main panel.

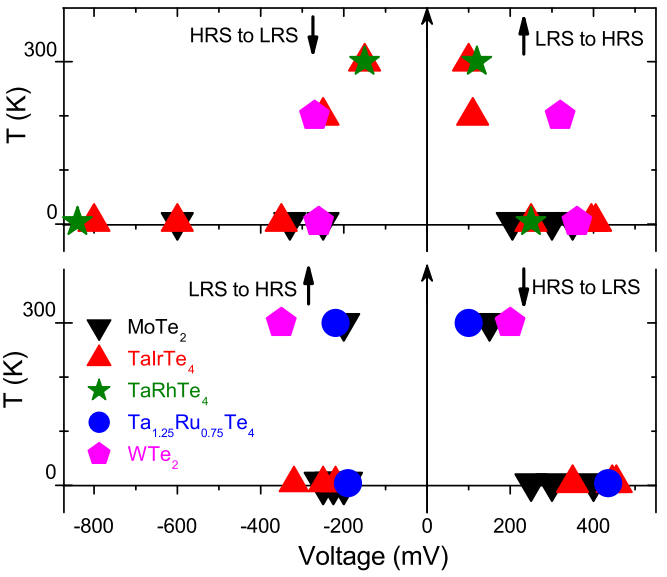

FIG. 3. Distribution of the switching voltages for different PCs with studied compounds between helium and room temperature. Upper (bottom) panel shows PCs where switching from LRS (HRS) to HRS (LRS) takes place at positive (negative) voltage. Switching voltages for LRS to HRS transition are marked by up arrows, and those for HRS to LRS transition are marked by down arrows. Switching voltages for two PCs at 200 K are shown in the upper panel.

analogous transition at helium temperature is quite sharp (see, e.g., Fig. 1). This could be due to enhanced fluctuation at the structural transition at higher temperature. Figure 2 shows dV/dI for the same PC measured with a time interval of about 12 h to demonstrate the stability of the switching effect under ambient conditions. The stability of the switching effect over one week at room temperature is shown in Fig. S1 in the Supplemental Material [22].

Similar switching effects were observed also for $TaRhTe_4$ and $Ta_{1.26}Ru_{0.75}Te_4$ (see Figs. S2 and S3 in the Supplemental Material [22]). "Hard" PCs, where instead of silver paint a thin Ag wire was used, also demonstrate a switching effect (see Figs. S3 and S4 in the Supplemental Material [22]). A disadvantage of "hard" PCs is their poor mechanical stability, thus most measurements were carried out on "soft" PCs.

Figure 3 summarizes the observed switching voltages for the LRS to HRS and HRS to LRS transitions for different PCs for all compounds at different temperatures. Most of the data presented are for $MoTe_2$ and $TaIrTe_4$ compounds (six PCs for each compound). First of all, it is seen that the polarity of each transition (LRS to HRS or HRS to LRS) can be positive or negative for different PCs with almost equal probability. For example, three PCs with $MoTe_2$ or $TaIrTe_4$ have an LRS to HRS transition at positive polarity, and three PCs have the opposite at negative polarity. However, if the switching occurs at a given polarity, then it is absent at the opposite polarity, at least in the same voltage range. Perhaps the atomic termination of the surface and the direction of the dipole moment (see Sec. III) play a role here. This point requires further investigation. Also, switching voltage has some distribution but is, on average, smaller at a higher temperature.

Finally, Fig. S5 in the Supplemental Material [22] demonstrates the detailed temperature dependence of dV/dI, where switching is manifested only close to room temperature. There, the lack of switching at a low temperature was connected with the need to apply a larger bias, while our setup has maximal current output of about 50 mA, therefore the maximal bias was limited by the low PC resistance. Detailed measurement of zero-bias resistance of this PC at different temperatures allowed us to estimate their size (analogously to the method used in the supplement of Ref. [9]) and, respectively, the electric field strength and current density. As a result, the estimated strength of an electric field at switching bias was about 2.5 times lower for this PC as compared to PC at helium temperature [see Fig. 1(d)]. It should be noted here that the estimation of the electric field gives a lower value, since we assume the formation of a single metallic contact or conducting channel. In the case of the formation of several PCs in parallel, their size will be smaller and the electric field will be correspondingly higher.

Note that dV/dI of $MoTe_2$ PC in the LRS [see, e.g., the black curve in Figs. 1(c) and 1(d)] has "metallic" behavior at low voltages, which transforms to the "semiconducting-like" decrease of dV/dI at higher bias [see also Figs. S5(a) and S5(b) for more details] producing a distinct maximum in dV/dI around 200 mV, similar to what we observed in the case of WTe_2 [9]. Interestingly, the transition to the "semiconducting-like" behavior was observed in the temperature dependence of resistance of a 6-nm-thick $MoTe_2$ sample at around 200 K (see Fig. 4S in the supplement of Ref. [23]). It seems that the size reduction (or thinning) promotes the emergence of "semiconductor-like" behavior in $MoTe_2$.

III. DISCUSSION

A switching effect in TMT has been reported recently by Zhang *et al.* [13] in "vertical devices made of $MoTe_2$ and $Mo_{1-x}W_xTe_2$ ($x < 0.1$) layers" (from 6 to 36 nm thick)

sandwiched between metallic electrodes. Zhang *et al.* [13] attributed the effect to the formation of a conductive filament with a transient structure (named $2H_d$) by applying an external electrical field. They considered the new phase $2H_d$ as a distorted $2H$ phase, the electrical properties of which can range from semiconducting to metallic. Zhang *et al.* [13] put forward that $MoTe_2$ (or $Mo_{1-x}W_xTe_2$) undergoes a reversible structural transition from a semiconducting $2H$ to a high (or more) conductive $2H_d$ state. Datye *et al.* [14] reported the observation of a similar switching in a structure containing layered $MoTe_2$ (10–55 nm thick) sandwiched between Au electrodes, using scanning thermal microscopy. They concluded that the switching "is likely caused by the breaking and forming of Au conductive plugs between the electrodes" when significant Joule heating promotes Au migration.

In our work, we used "bulk" samples with a thickness of about 100 μm to create PCs. The observed "bipolar" switching from the LRS to the HRS occurs only at definite polarity above a definite threshold. We would like to emphasize that in contrast to the previous works, each of our measurements starts from the "metallic" ground state (marked by "*s*" in the figures) and undergoes the transition to the highly resistive "semiconducting"-type state if the applied voltage is above some threshold. This eliminates, for example, Ag filament formation as a possible reason for the switching to HRS. We have also tried to start from the semiconducting $2H$-phase of $MoTe_2$, but we observed no switching effect. This behavior, and the fact that observed "bipolar" switching from the LRS to HRS (and from the HRS to LRS) occurs only at definite polarity, testifies also to a nonthermal mechanism as a main driving force. Therefore, the nature of our effect is different from resistive switching described by Zhang *et al.* [13] and Datye *et al.* [14]. Of course, the temperature can play some role, while, for example, the switching voltage and amplitude depend on the temperature (see Fig. 3). However, the electric field is the primary reason for the switching.

Further, as Figs. 1(c) and 1(d) and Figs. S4 and S5 (a,b) show, the high (or more) conductive state (referred to here as LRS) demonstrates metallic behavior. In this case, dV/dI increases with voltages, forming a minimum at zero-bias. Hence, in our case, the LRS corresponds to the semimetallic T_d phase, and the low conductive state (or HRS) with a sharp zero-bias maximum in the dV/dI is created due to an applied voltage. This may be because of the formation of a distorted state in the PC core or due to enhanced resistance at the domain wall between the PC core and the bulk with opposite polarity, which were discussed in [15,16,24] with respect to $MoTe_2$ and WTe_2. The domain formation in the PC can be caused by a high electric field in its core [see Fig. 4(a)]. That is quite possible, given the fact that, according to a recent observation, native metallicity and ferroelectricity can coexist in $MoTe_2$ and WTe_2 [15,16,24].

Yuan *et al.* [16] relate the origin of the ferroelectricity in the $MoTe_2$ monolayer to spontaneous symmetry breaking due to relative displacements of Mo atoms and Te atoms as a result of the formation of a distorted $d1T$ phase. Fei *et al.* [15] observed that two- or three-layer WTe_2 exhibits spontaneous out-of-plane electric polarization that can be switched using gate electrodes. Moreover, Sharma *et al.* [24] provide evidence that native metallicity and ferroelectricity coexist also in a bulk

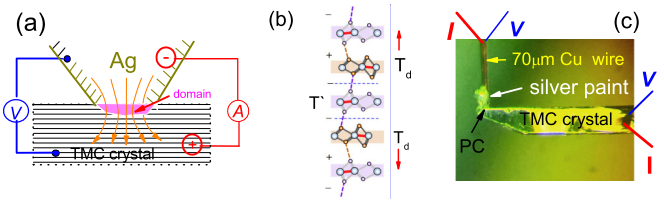

FIG. 4. Representation of the PC. (a) Model of PC between TMT crystal and Ag-tip showing current and voltage leads and "domain," where an electric field is maximal. Arrows show spreading of a current in PC. (b) Schematic model of domain wall between $T_d\uparrow$ and $T_d\downarrow$ states containing one $1T'$ unit as bridge according to [25]. (c) Photoimage of "soft" PC, where silver paint touches the sample and connects to a thin Cu wire Ø70 μm. The Cu wire and the sample are connected to an electrical circuit by *I* and *V* leads.

crystalline WTe_2. They have also demonstrated that WTe_2 has switchable spontaneous polarization and natural ferroelectric domains with a distorted circular profile from 20 to 50 nm. That is, ferroelectricity is a bulk property of WTe_2 and is not limited to few-layer samples only.

Therefore, we assume that when relative atomic displacements of Mo/W atoms and Te atoms produce polarization (in other words, an electric field), then the inverse effect must also take place. Namely, a high electric field in a PC can induce the mentioned atomic displacement that leads to the new phase formation and the appearance of a ferroelectric domain in the PC [see Fig. 4(a)] with different structure. In this case, the new phase (something like distorted $d1T$) must manifest "semiconducting-like" behavior. Then, the observed switching created in the PC core domain can be due to reversible phase transition between distorted or intermediate (possible $d1T$) phase and semimetallic T_d or $1T'$ phase triggered by a high electric field.

Considering that the materials investigated in this work belong to the family of Weyl semimetals with topologically protected surface states, the discovery and exploitation of the specific properties of these surface states in homo/heterostructures is a great challenge. Note that the investigated materials have the same T_d crystal structure at low temperatures, which has broken inversion symmetry. This leads to an uncompensated dipole, resulting in polarization along the *c*-axis, which can exist in the $T_d\uparrow$ and $T_d\downarrow$ states due to the asymmetric Te bonding environments [25]. Imagine that under the action of high electric field, the domain [see Fig. 4(a)] has a certain polarization, let us say $T_d\uparrow$. Therefore, a high electric field of opposite polarity can flip the dipole moment of the domain with the corresponding change of the crystal structure from $T_d\uparrow$ to $T_d\downarrow$. The interface between $T_d\uparrow$ and $T_d\downarrow$ is T' phase [see Fig. 4(b)]. Thus, the electron scattering on the domain wall between $T_d\uparrow$ and $T_d\downarrow$ phase with specific surface states can lead to the increased resistance and simulate HRS behavior. Of course, this model requires sophisticated theoretical calculations that have not yet been completed.

It should be recalled here that the *dI/dV* at HRS displays a linear behavior [see the inset of Fig. 1(c), and Figs. S6, S7, and S8 in the supplemental material [22]). At the same time, the dV/dI has also a logarithmic behavior for a certain bias

range (see Figs. S6, S7, and S8 in the Supplemental Material [22]). This observation is interesting and it must be considered when developing a theory for the switching effect.

IV. CONCLUSION AND OUTLOOK

We report a resistive switching in point contacts (PCs) based on a series of TMT compounds such as $MeTe_2$ (Me = Mo, W) and Ta$MeTe_4$ (Me = Ru, Rh, Ir). The switching effect consists of up to two orders of magnitude change in the PC resistance, which increases with the lowering of temperature. All the investigated compounds are layered van der Waals materials, which have the same crystal structure, namely T_d phase. The T_d phase has broken inversion symmetry. It means that even these materials are semimetals, nevertheless each layer has a dipole moment. Since the layers are weakly coupled by the van der Waals forces, the external electric fields can interact with the dipole moment, causing a transition to another state. In addition, the presence of domain walls with topological interfacial states can also play a role. Undoubtedly, this simple method of device preparation has a great advantage in finding suitable materials, and it can be used, at least, to look for the resistive switching effect before functionalizing them in nanoelectronic application. It is worth noting here that the first observation of the resistive switching effect, e.g., in strongly correlated high-T_c materials [26] and manganese-based perovskite oxides with collosal magnetoresistance [27], was also observed by using the PC technique, demonstrating its capabilities. Summing up, our observation of the resistive switching effect in a series of TMT compounds expands significantly the range of materials that are promising for RRAM development [13,28], for ferroelectric phase-change transistors [29], and for other nanoelectronic applications [30]. On the one hand, this paves the way for discovering the effect in other metallic layered materials, leading to electronics with advanced functionalities. On the other hand, to understand the underlying physics of the switching processes is of great importance, which can open the avenue to application of topological surface states.

V. EXPERIMENTAL SECTION

Synthesis. Bulk single crystals of $MoTe_2$, WTe_2, and Ta$MeTe_4$ (Me = Ru, Rh, Ir) compounds were grown with Te flux. To avoid contamination, the mixing and weighting were carried out in an Ar-filled glove box. In the case of the crystal growth of $MoTe_2$ and WTe_2, 0.5 g of Mo (or W) powder and 10 g Te were mixed and placed in an evacuated quartz ampoule. The ampoule was placed in a box furnace and slowly heated to 1000 °C and cooled down slowly to 800 °C followed by a hot centrifuge to remove the excess Te-flux. A similar approach was used by us for the growth of the Ta$MeTe_4$ (Me = Ru, Rh, Ir) family [21]. Single crystals were grown having a needlelike shape with a layered morphology. The as-grown crystals were characterized by SEM in EDX mode for compositional analysis and by x-ray diffraction for structural analysis. More details of the crystal growth and characterization are reported in Refs. [6,21,31].

Point-contact spectroscopy. PCs were prepared by touching a thin Ag wire to a room-temperature-cleaved flat surface of TMT needlelike single-crystal flake or contacting its edge by this wire. The calculated diameter of the point contact is of the order of 100–300 nm. So-called "soft" PCs were made by dripping a small drop of silver paint onto the cleaved TMT surface/edge [see Fig. 4(c)]. The latter type of PCs demonstrate better stability versus temperature change. Thus, we conducted resistive measurements on the heterocontacts between a normal metal (Ag or silver paint) and the TMT. We measured current-voltage characteristics ($I-V$ curves) of PCs and their first derivatives $dV/dI(V)$. The first derivative or differential resistance $dV/dI(V) \equiv R(V)$ was recorded by scanning the dc current I on which a small ac current i was superimposed using a standard lock-in technique. The measurements were performed in the temperature range from liquid helium up to room temperature.

ACKNOWLEDGMENTS

We thank A. V. Terekhov and S. Gaβ for technical assistance. This work was financially supported by the Volkswagen Foundation in the frame of Trilateral Initiative. Y.G.N., D.L.B., and O.E.K. are grateful for support by the National Academy of Sciences of the Ukraine under project Φ4-19, and would like to thank the IFW Dresden for hospitality. S.A. acknowledges the support by Deutsche Forschungsgemeinschaft (DFG) through Grant No. A.S. 523/4-1. S.A., B.B., and D.E. also acknowledge the support of DFG through Projekt No. 405940956.

[1] S. Manzeli, D. Ovchinnikov, D. Pasquier, O. V. Yazyevand, and A. Kis, Nat. Rev. Mater. **2**, 17033 (2017).

[2] B. Yan and C. Felser, Annu. Rev. Condens. Matter Phys. **8**, 337 (2017).

[3] Q. H. Wang, K. Kalantar-Zadeh, A. Kis, J. N. Coleman, and M. S. Strano, Nat. Nanotech. **7**, 699 (2012).

[4] M. N. Ali, J. Xiong, S. Flynn, J. Tao, Q. D. Gibson, L. M. Schoop, T. Liang, N. Haldolaarachchige, M. Hirschberger, N. P. Ong, and R. J. Cava, Nature (London) **514**, 205 (2014).

[5] S. Thirupathaiah, R. Jha, B. Pal, J. S. Matias, P. Kumar Das, P. K. Sivakumar, I. Vobornik, N. C. Plumb, M. Shi, R. A. Ribeiro, and D. D. Sarma, Phys. Rev. B **95**, 241105(R) (2017).

[6] S. Khim, K. Koepernik, D. V. Efremov, J. Klotz, T. Förster, J. Wosnitza, M. I. Sturza, S. Wurmehl, C. Hess, J. van den Brink, and B. Büchner, Phys. Rev. B **94**, 165145 (2016).

[7] Y. Qi, P. G. Naumov, M. N. Ali, C. R. Rajamathi, W. Schnelle, O. Barkalov, M. Hanfland, S.-C. Wu, C. Shekhar, Y. Sun, V. Süß, M. Schmidt, U. Schwarz, E. Pippel, P. Werner, R. Hillebrand, T. Förster, E. Kampert, S. Parkin, R. J. Cava, C. Felser, B. Yan, and S. A. Medvedev, Nat. Commun. **7**, 11038 (2016).

[8] Yu. G. Naidyuk, O. E. Kvitnitskaya, D. L. Bashlakov, S. Aswartham, I. V. Morozov, I. O. Chernyavskii, G. Fuchs, S.-L. Drechsler, R. Hühne, K. Nielsch, B. Büchner, and D. V. Efremov, 2D Mater. **5**, 045014 (2018).

[9] Yu. G. Naidyuk, D. L. Bashlakov, O. E. Kvitnitskaya, S. Aswartham, I. V. Morozov, I. O. Chernyavskii, G. Shipunov, G. Fuchs, S.-L. Drechsler, R. Hühne, K. Nielsch, B. Büchner, and D. V. Efremov, 2D Mater. **6**, 045012 (2019).
[10] F. Tang, H. C. Po, A. Vishwanath, and X. Wan, Nat. Phys. **15**, 470 (2019).
[11] M. Ezawa, Sci. Rep. **9**, 5286 (2019).
[12] Z. Wang, B. J. Wieder, J. Li, B. Yan, and B. A. Bernevig, Phys. Rev. Lett. **123**, 186401 (2019).
[13] F. Zhang, H. R. Zhang, S. Krylyuk, C. A. Milligan, Y. Q. Zhu, D. Y. Zemlyanov, L. A. Bendersky, B. P. Burton, A. V. Davydov, and J. Appenzeller, Nat. Mater. **18**, 55 (2019).
[14] I. Datye, M. M. Rojo, E. Yalon, S. Deshmukh, M. J. Mleczko, and E. Pop, Nano Lett. **20**, 1461 (2020).
[15] Z. Fei, W. Zhao, T. A. Palomaki, B. Sun, M. K. Miller, Z. Zhao, J. Yan, X. Xu, and D. H. Cobden, Nature (London) **560**, 336 (2018).
[16] S. Yuan, X. Luo, H. L. Chan, C. Xiao, Y. Dai, M. Xie, and J. Hao, Nat. Commun. **10**, 1775 (2019).
[17] N. A. Benedek and T. Birol, J. Mater. Chem. C **4**, 4000 (2016).
[18] Yu. G. Naidyuk and I. K. Yanson, *Point-Contact Spectroscopy*, Springer Series in Solid-State Sciences Vol. 145 (Springer, New York, 2005).
[19] B. I. Verkin, I. K. Yanson, I. O. Kulik, O. I. Shklyarevski, A. A. Lysykh, and Yu. G. Naydyuk, Solid State Commun. **30**, 215 (1979).
[20] D. A. Rhodes, A. Jindal, N. F. Yuan, Y. Jung, A. Antony, H. Wang, B. Kim, Y. u-c. Chiu, T. Taniguchi, K. Watanabe, K. Barmak, L. Balicas, C. R. Dean, X. Qian, L. Fu, A. N. Pasupathy, and J. Hone, Nano Lett. **21**, 2505 (2021).
[21] G. Shipunov, B. R. Piening, C. Wuttke, T. A. Romanova, A. V. Sadakov, O. A. Sobolevskiy, E. Yu. Guzovsky, A. S. Usoltsev, V. M. Pudalov, D. Efremov, S. Subakti, D. Wolf, A. Lubk, B. Büchner, and S. Aswartham, J. Phys. Chem. Lett. **12**, 6730 (2021).
[22] See Supplemental Material at http://link.aps.org/supplemental/10.1103/PhysRevMaterials.5.084004 for detailed stability of the switching effect and more supporting figures.
[23] C. Cao, X. Liu, X. Ren, X. Zeng, K. Zhang, D. Sun, S. Zhou, Y. Wu, Y. Li, and J.-H. Chen, 2D Mater. **5**, 044003 (2018).
[24] P. Sharma, F.-X. Xiang, D.-F. Shao, D. Zhang, E. Y. Tsymbal, A. R. Hamilton, and J. Seidel, Sci. Adv. **5**, eaax5080 (2019).
[25] F.-T. Huang, S. J. Lim, S. Singh, J. Kim, L. Zhang, J.-W. Kim, M.-W. Chu, K. M. Rabe, D. Vanderbilt, and S.-W. Cheong, Nat. Commun. **10**, 4211 (2019).
[26] L. F. Rybaltchenko, N. L. Bobrov, V. V. Fisun, I. K. Yanson, A. G. M. Jansen, and P. Wyder, Eur. Phys. J. B **10**, 475 (1999).
[27] M. A. Belogolovskii, Y. u. F. Revenko, A. Yu. Gerasimenko, V. M. Svistunov, E. Hatta, G. Plitnik, V. E. Shaternik, and E. M. Rudenko, Low Temp. Phys. **28**, 391 (2002).
[28] Q. Zhao, Z. Xie, Y.-P. Peng, K. Wang, H. Wang, X. Li, H. Wang, J. Chen, H. Zhang, and X. Yan, Mater. Horiz. **7**, 1495 (2020).
[29] W. Hou, A. Azizimanesh, A. Sewaket, T. Peca, C. Watson, M. Liu, H. Askari, and S. M. Wu, Nat. Nanotech. **14**, 668 (2019).
[30] J. Su, K. Liu, F. Wang, B. Jin, Y. Guo, G. Liu, H. Li, and T. Zhai, Adv. Mater. Interfaces **6**, 1900741 (2019).
[31] A.-S. Pawlik, S. Aswartham, I. Morozov, M. Knupfer, B. Büchner, D. V. Efremov, and A. Koitzsch, Phys. Rev. Mater. **2**, 104004 (2018).